

〈Technical Note〉

**3-D CFD Analysis of the CANDU-6 Moderator Circulation
Under Normal Operating Conditions**

Churl Yoon, Bo Wook Rhee, and Byung-Joo Min

Korea Atomic Energy Research Institute
150 Deokjin-dong, Yuseong-gu, Daejeon 305-353, Korea

cyoon@kaeri.re.kr

(Received April 9, 2004)

Abstract

A computational fluid dynamics model for predicting moderator circulation inside the Canada deuterium uranium (CANDU) reactor vessel has been developed to estimate the local subcooling of the moderator in the vicinity of the calandria tubes. The buoyancy effect induced by the internal heating is accounted for by the Boussinesq approximation. The standard k- ϵ turbulence model with logarithmic wall treatment is applied to predict the turbulent jet flows from the inlet nozzles. The matrix of the calandria tubes in the core region is simplified to a porous media in which the anisotropic hydraulic impedance is modeled using an empirical correlation of pressure loss. The governing equations are solved by CFX-4.4, a commercial CFD code developed by AEA technology. The resultant flow patterns of the constant-z slices containing the inlet nozzles and the outlet port are "mixed-type," as observed in the former 2-dimensional experimental investigations. With 103% full power for conservatism, the maximum temperature of the moderator is 82.9°C at the top of the core region. Considering the hydrostatic pressure change, the minimum subcooling is 24.8°C.

Key Words : CANDU-6, wolsong units 2/3/4, moderator circulation, CFD, subcooling

I. Introduction

For some loss of coolant accidents with a coincident loss of emergency core cooling in a CANDU reactor, the fuel channel integrity depends on the capability of the moderator to act as the ultimate heat sink. Predicting the temperature distributions of the moderator inside the calandria vessel under LOCA transients is a

critical issue in CANDU safety. A CFD model based on the CFX-4 code for predicting the moderator temperature during these accidents is under development in Korea while the Canadian nuclear industry currently uses the MODTURC_ÇLAS, a specialized CFD code for moderator circulation, for licensing and safety analysis. The objectives of this study are to develop a CFD model for predicting CANDU-6 moderator

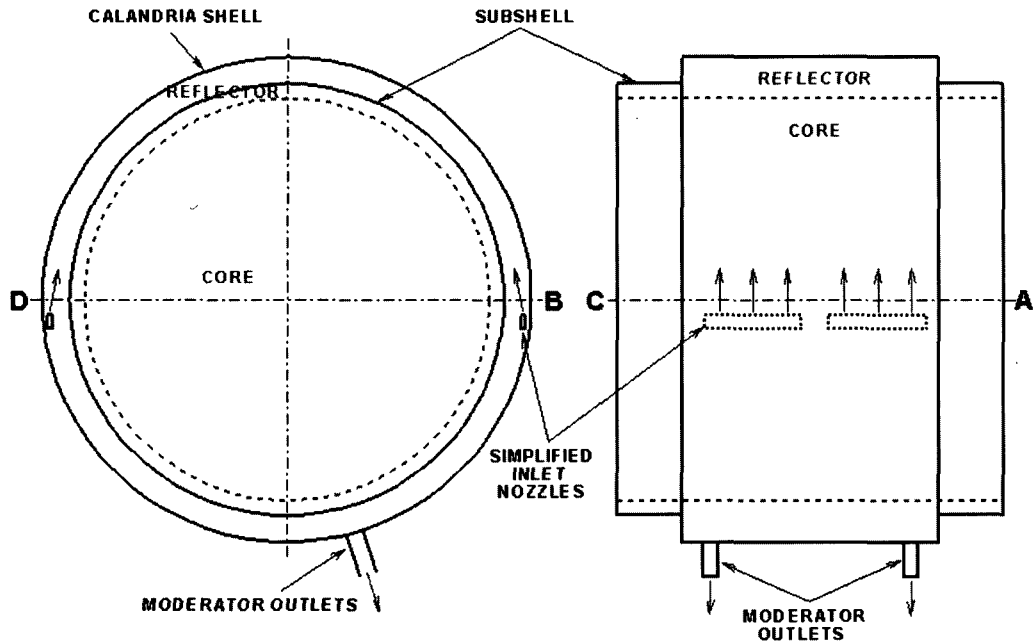


Fig. 1. Simplified View of the CANDU-6 Calandria Vessel

temperatures, and to predict the steady-state velocity field and temperature distribution of the Wolsong Units 2, 3, & 4 moderators under normal operating conditions.

Figure 1 illustrates a simplified cutaway view of the CANDU-6 calandria vessel. The calandria vessel is an indented cylinder that is 6.0 m long with a main-shell diameter of 7.60 m and a sub-shell diameter of 6.76 m. Each of the sub-shells has a length of 0.97 m. In addition to a matrix of 380 calandria tubes in the core region of the vessel, there are a number of horizontal and vertical reactivity mechanisms, which are omitted in the current CFD model for the sake of simplicity. The moderator fluid is heavy water at about an atmospheric cover pressure. The moderator fluid is extracted from the vessel through two outlet ports located at the bottom of the vessel. The two outlet ports are symmetrically located in the axial direction, but are asymmetrically placed in the circumferential

direction. After discharging through the outlet ports, the fluid mixes in a header, passes through one of the two operating pumps to be cooled via the parallel heat exchangers, and is returned to the calandria vessel through the eight inlet nozzles located at the side of the vessel. Two inlet nozzles are modeled as one simplified rectangular block and the inlet velocities are set uniform in this study. Moderator simulations with a more detailed inlet nozzle model and inlet velocity profile are scheduled for future studies. The inlet nozzles are symmetrically placed in the x-y plane with respect to the vertical centerline but are asymmetrically placed in the axial direction.

Carlucci and Cheung [1] investigated a two-dimensional flow of internally heated fluid in a circular vessel to study the flow patterns inside the calandria vessel. There was a matrix of heating pipes at the center region of the circular vessel. The vessel had two inlet nozzles at the sides and outlets at the bottom. It was observed that the flow

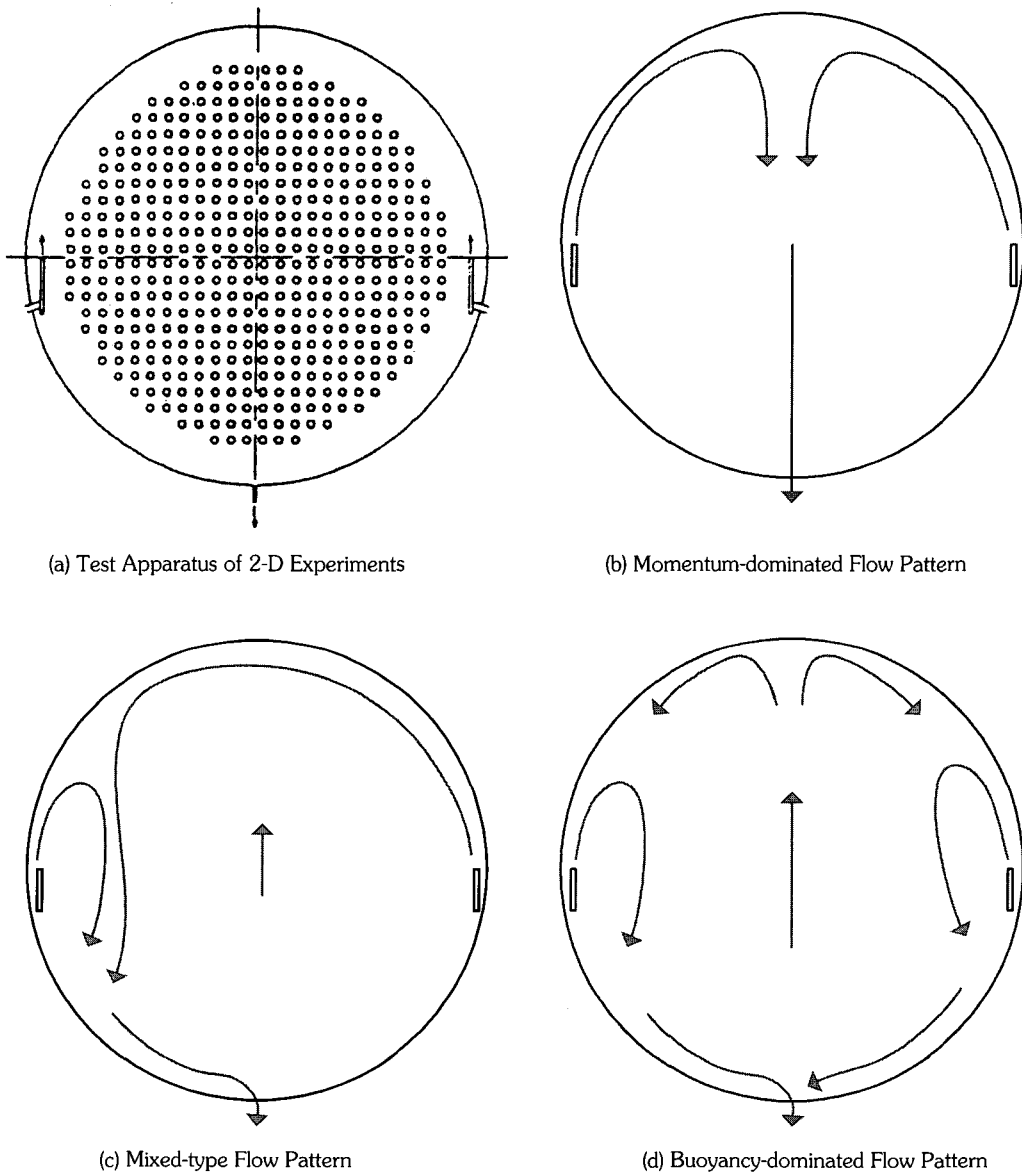


Fig. 2. Three Flow Patterns of the CANDU-6 Moderator Circulation in the 2-D Experiments

pattern inside the circular vessel was determined by the ratio of characteristic buoyancy to inertia forces, the non-dimensional Archimedes (Ar) number, for the given geometry. Two distinct types of flow patterns were observed: jet-momentum dominated for a low Ar and buoyancy dominated for a high Ar . The transition range of

the Ar number represented a 'mixed-type' flow pattern between the jet-momentum-dominated and buoyancy-dominated flow patterns. It was also observed that the resultant steady-state flow pattern could oscillate periodically between the buoyancy-dominant flow and the momentum-dominated flow in the condition of a certain range

of the Archimedes number.

Huget et al. [2, 3] investigated experimentally the moderator circulation and temperature distribution of the CANDU moderator under normal operating conditions, as well as under other conditions, using a 2-dimensional moderator circulation facility at the Stern Laboratories. The cross section of this facility was a 1/4 scale of a real calandria vessel, while the geometry and flow conditions were uniform in the axial direction. They [6] also provided the predicted velocity fields and temperature distributions for each test case, using MODTURC and MODTURC-CLAS (MODerator TURbulent Circulation Co-Located Advanced Solution).

Figure 2 shows the three clearly classified flow patterns observed during the 2-dimensional moderator circulation experiments at the Stern Laboratories: momentum-dominated, mixed-type, and buoyancy-dominated flow patterns. Without a heat load in the core region, the flow pattern is momentum-dominated (Fig. 2 (b)). With a high heat load in the core region, the strong buoyancy-driven upward flow suppresses the cold injected fluid and the flow pattern is buoyancy-dominated (Fig. 2 (d)). The mixed-type flow pattern (Fig. 2 (c)) is an intermediate flow pattern between the momentum-dominated and the buoyancy-dominated patterns. If one starts with a momentum-dominated flow pattern and increases the heat load in the core region gradually, the downward flows conflict with the increasing buoyancy forces in the core region. When the buoyancy force reaches a certain threshold level, the downward fluid tilts to one side so that the flow pattern becomes asymmetric. At this moment, inlet jet reversal occurs near the top. If the heat load is further increased, the inlet jet reversal angle decreases from 90° and, at a certain high heat load level, the flow pattern changes from a momentum-dominated to a

buoyancy-dominated pattern.

In 1995, Collins [4, 5] performed a moderator circulation analysis under normal operating conditions for Wolsong 2, 3, & 4 using the PHOENICS2 computer code, which is a 3-D moderator simulation applied to real CANDU reactors. It was concluded that a steady-state solution could not be reached and that only quasi-steady solutions could be achieved. It was also reported that a fully converged steady state solution had been obtained when the inlet velocity was increased by a factor of 1.5 (~3.0 m/s). In this quasi-steady solution, the maximum temperature within the moderator over a period of 0~300 s varies between 78.5°C, the lowest value, and 81.7°C, the highest value.

2. Model Description

For thermal hydraulic analysis of the CANDU-6 moderator, the general-purpose CFD code, CFX-4.4 (AEA Technology), is used to coincidentally solve a continuity equation, the momentum equations, and an energy equation. The finite-volume method is used. The advection terms are discretized by the first-order accurate Hybrid differencing scheme, while the centred differencing schemes are used for the other terms. The flow is assumed to be steady, incompressible, and single-phase. The SIMPLEC algorithm is used, which is recommended for a flow with a strong buoyancy effect. The Boussinesq approximation is applied to the buoyancy forces in which the density in the momentum source term is a linear function of temperature and is constant in the other terms of the governing equations. The standard k-turbulence model with logarithmic wall treatment is used, as the flow field is known to be turbulent. CFX-4.4 uses a body-fitted grid with Rhie-Chow interpolation rather than a staggered grid to effectively simulate the three-dimensional fluid flow

in complex geometries.

The matrix of the calandria tubes in the core region is simplified by the porous media approach [6]. The hydraulic resistance experienced by the fluid flowing through the core region is accounted for as source terms of the momentum equations. In the prediction of the local minimum subcooling of the CANDU-6 moderator under normal operating conditions and LOCA transients, the resultant velocity fields and temperature predictions are very sensitive to the hydraulic resistance correlations for the porous region that represents the matrix of the calandria tubes.

2.1. Grid Structures

Radial-shaped grid structures that look like cylindrical coordinates are selected for the simulation. In selecting the grid structures, the important factors to consider are computing cost, discretization error, and assumptions related to grid spacing such as the porous media approach. Considering these factors, the radial-shaped grid

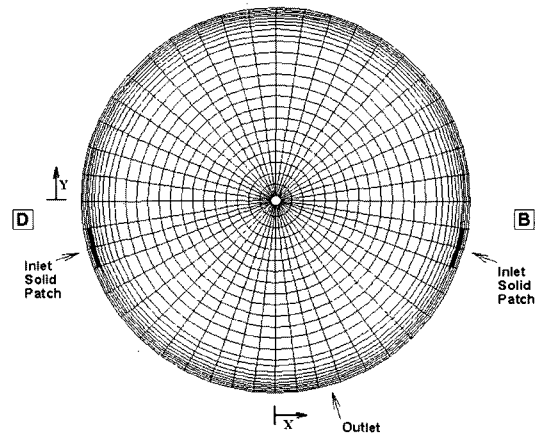


Fig. 4. Radial and Angular Grid (View from pressurizer or "C")

structures may not be the best choice, so future analyses will use a butterfly-shaped grid, such as the one that has been used in recent studies by Canadian researchers. Figures 3 and 4 show the multi-block structured grid used in this simulation. The computational grid consisted of 46 angular, 16 radial, and 19 axial divisions in the first block, and 46 angular, 8 radial, and 15 axial divisions in the second block. The number of the total computational cells is 19,504. An adiabatic pipe is assumed to exist at the location of the central z-axis of the solution domain to keep all the grid structures hexahedral and to avoid singularity. Simple tests proved that the existence of this imaginary pipe would not affect the overall trend of moderator circulation or temperature distribution. The grid-independency has not been achieved.

2.2. Hydraulic Resistance for a Porous Media

Hydraulic resistance consists of form drag and friction drag. If hydraulic resistance were not dependent on the attack angle between the flow direction and tube axis, the moderator fluid flow could be decomposed conveniently into an axial flow and a lateral flow.

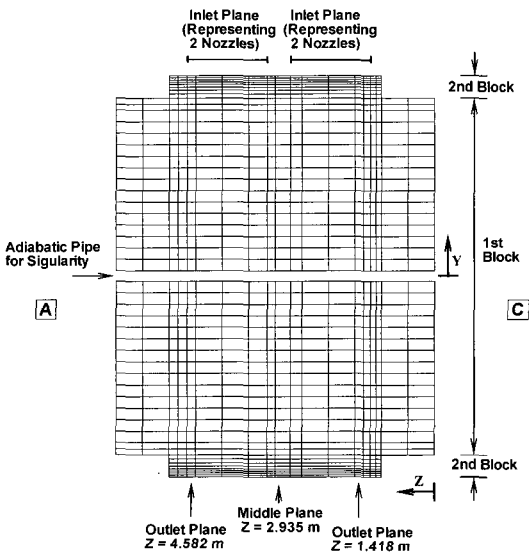


Fig. 3. Axial and Radial Grid (View from moderator pumps or "D")

For the axial flow, there is no form drag. If one assumes that the fluid velocities can be decomposed into the x, y, and z components, the hydraulic resistance of the axial flow could be expressed by the conventional correlations of frictional pressure loss in a cylindrical pipe.

$$\left. \frac{\Delta P}{\Delta L} \right)_z = \frac{\Delta P_{fric}}{\Delta z} = \frac{f \rho u_z^2}{2D_e} \quad (1)$$

where

ΔP_{fric} = frictional pressure loss (N/m²),

Δz = axial unit length (m),

f = friction factor,

ρ = density (kg/m³),

u_z = axial component of velocity (m/sec),
and

D_e = hydraulic diameter of axial flow passage (m).

Friction factor, f , is calculated from the friction factor correlation for the flow inside the circular pipes. For the turbulent flow of a low Reynolds number,

$$f = 0.316 \cdot \text{Re}^{-0.25} \quad (2)$$

Here, the Reynolds number Re is defined by $u_z D_e / \nu$ and ν is kinematic viscosity in m²/sec.

For the transverse (lateral) flow across the tube bank, Hadaller et al. [7] investigated the pressure drop of the fluid flows crossing the staggered and in-line tube banks, in which the Reynolds number range was 2,000 to 9,000 and the pitch to tube diameter ratio was 2.16. Also, they concluded that for the given p/D ratio, the effect of the staggering is not significant. From this experimental investigation, the empirical correlation for the pressure loss coefficient is obtained as

$$\text{PLC} \equiv \frac{\Delta P}{N_r \cdot \rho \cdot \frac{V_m^2}{2}} = 4.54 \cdot \text{Re}^{-0.172}, \quad (3)$$

Where

P = pressure (N/m²),

N_r = number of rows, and

V_m = free-stream velocity before obstruction.

The hydraulic resistance source terms in the momentum equations are in the form of a pressure drop per unit length.

$$\frac{\Delta P}{\Delta L} = \frac{N_r}{\Delta L} 4.54 \cdot \text{Re}^{-0.172} \cdot \rho \cdot \frac{V_m^2}{2} \quad (4)$$

Here, $N_r/\Delta L$ can be expressed as an inverse of the row spacing of the tube bank and the Reynolds number is defined as $V_m D/\nu$. Here, D (= 0.131 m) is the calandria tube diameter. Note that V_m is the velocity before entering the tube bank and that V_m is different from the local moderator velocity in the core region of the CANDU calandria vessel, V_c . When one defines γ_A as area porosity,

$$V_m = \gamma_A V_c \quad (5)$$

Decomposition of the pressure gradient per unit travel length gives

$$\left. \left(\frac{\Delta P}{\Delta L} \right)_x = \frac{\Delta P}{\Delta L} \cos \theta = \frac{\Delta P}{\Delta L} \cdot \frac{u_x}{V_c} \quad (6)$$

$$\left. \left(\frac{\Delta P}{\Delta L} \right)_y = \frac{\Delta P}{\Delta L} \sin \theta = \frac{\Delta P}{\Delta L} \cdot \frac{u_y}{V_c} \quad (7)$$

with θ as the angle between the fluid velocity vector and the x-axis.

Now, Eq. (4) can be implemented as below.

$$\left. \left(\frac{\Delta P}{\Delta L} \right)_i = \frac{1}{\Delta L_{row}} \cdot 4.54 \cdot \left(\frac{\gamma_A V_c D}{\nu} \right)^{-0.172} \cdot \rho \cdot \frac{(\gamma_A^2 V_c^2)}{2} u_i \quad (8)$$

where ΔL_{row} is the row spacing and the subscript i denotes the x or y component.

Eqs. (1) and (8) are inserted into the momentum equations for the core region as source terms to

represent the hydraulic resistance of the tube bank matrix.

The hydraulic resistance correlation used in this study underestimates the axial resistance, because this resistance model was established based on cross flow correlations only. An improved 3-dimensional hydraulic resistance model will be developed with experimental data for the flows across inclined tube banks.

2.3. Heat Load for the Moderator Under Normal Operating Conditions

For the 2064MW(th) nuclear reactor, the nuclear energy deposited in the moderator from the gammas and neutrons is 78.7 MW and the total energy deposition in the reflector is 5.9 MW at full power. Table 1 summarizes the moderator system heat load during steady-state operations at full power, as calculated from physical studies that used the ANISN code [8]. Under normal operating

Table 1. Moderator System Heat Load During Steady State Operations at a Full Power [Ref. 8]

Componet	Heat Load(MW)
Heat generated in	
a) Moderator	78.7
b) Reflector	5.9
c) Calandria Tubes	4.3
d) Guide Tubes and Reactivity Mechanisms	2.7
Heat transfer from	
a) Calandria Shell and Tubesheets	1.7
b) Fuel Channels	3.0
Heat loss from	
a) Moderator pipings	- 0.3*
Heat gain from	
a) Moderator pumps	0.7
TOTAL	96.7 MWth

* Negative sign indicates heat loss.

conditions, direct heating of the gammas and neutrons generates most of the heat load to the moderator while heat conduction and convection accounts for only a small portion of the total heat load.

For a conservative analysis, the total heat load to the moderator is taken to be 103 MW (103%), consisting of 96.7 MW to the core and 6.3 MW to the reflector region. The spatial heat distribution of the core region is calculated based on the actual power map. Figure 5 shows the time-averaged axial power distribution for the M11 channel and its fitting equation. The axial power distributions of most channels follow a sine shape, while some indentations appear in certain axial power distributions because of the existence of controlling devices. We assumed that the 4-th order polynomial fit of channel M11 represents all the axial power distributions. This assumption should be examined at the application stage after this developing procedure. Figure 6 shows the time-averaged radial power distribution data and their fitting equation. From the power map, it is found that the trends in all the radial outward directions are almost the same (symmetric). Thus, only one radial fitting equation is found and it is

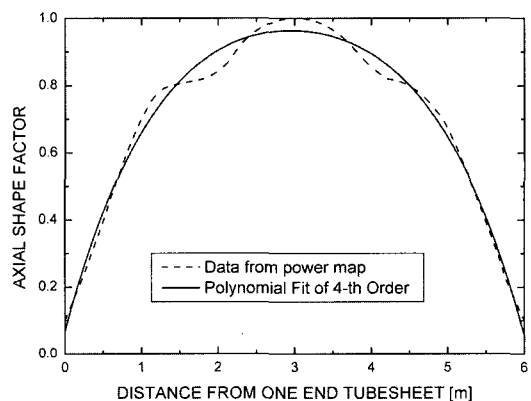


Fig. 5. Time-Averaged Axial Power per Unit Volume of the M11 Channel and the 4-th Order Polynomial Fit

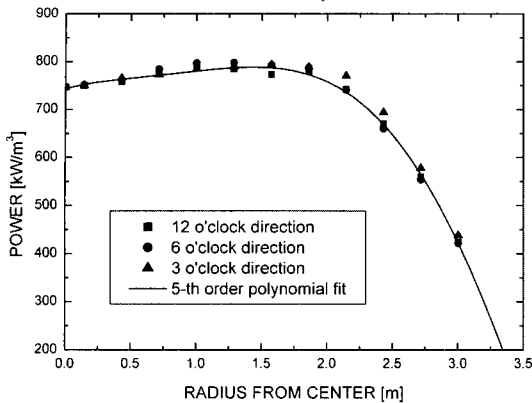


Fig. 6. Time-Averaged Radial Power Distribution and the 5-th Order Polynomial Fit

angle-independent. For simplicity, the power distribution in the reflector region was assumed to be uniform, and was maintained at 6.1% of the heat load to the moderator due to the fission product decay and neutronic power.

Service water to the heat exchangers is controlled by the Moderator Temperature Control (MTC) program to maintain the calandria moderator outlet temperature at 69.0°C. Under nominal full power conditions, the corresponding inlet temperature is set at 45.0°C. The average inlet coolant velocity is about 2 m/s at the nozzle entrance. The total flow rate through the eight nozzles is 940 L/s. The thermal boundary condition of the calandria outer wall is conservatively assumed to be adiabatic.

3. Moderator Circulation Under Normal Operating Conditions

This steady-state computation using CFX-4.4 was performed in an HP-C3600 workstation. The convergence criteria were the enthalpy residual reduction factor of 10^{-3} and the largest mass residual of 10^{-7} . Because the energy equation and

momentum equations are strongly interrelated in this computation, the algebraic multi-grid solver and false time stepping technique were adapted to accelerate the converging speed for the energy equation. The number of steady computation iterations was about 200,000 to 300,000.

The resultant velocity field and temperature distribution is presented in 3 slices of constant-z and 1 slice of constant-x. The z values of the constant-z slices were selected carefully. Therefore, two x-y planes include the inlet nozzles and an outlet port (Fig. 7 & 9), and the other constant-z slice contains neither a nozzle nor an outlet (Fig. 8), which represents the x-y plane between the inlets. The x value of the constant-x slice is 0.3 m (Fig. 10).

Figure 7 is the x-y plane in which $z = 1.418$ m away from one end tubesheet, where two inlet nozzles and an outlet port are sliced. In Fig. 7(a), the flow reversal is observed only for the injected fluid from the inlet nozzle far from the outlet port. The cold injected fluid from the inlet nozzle at the opposite side is guided by the upper circumferential vessel wall and goes all the way through the upper reflector region. The two injected fluids meet together at an angle of about 50° over the horizontal centerline, where the jet reversal occurs. The reversed fluid goes down to the bottom, guided by the circumferential lower vessel wall. This asymmetry of the flow pattern is induced by the interaction between the buoyancy forces and the inlet jet momentum forces. The velocity vectors in the core region are relatively small compared to those of the reflector region due to the hydraulic resistance in the core region. In Fig. 7(b), the temperature distribution shows a steep temperature change around the jet reversal area. In this area, the fluid that was heated during its journey from the other side of the nozzle suppresses the cold injected fluid. The hottest spot is located at the upper center area of the core

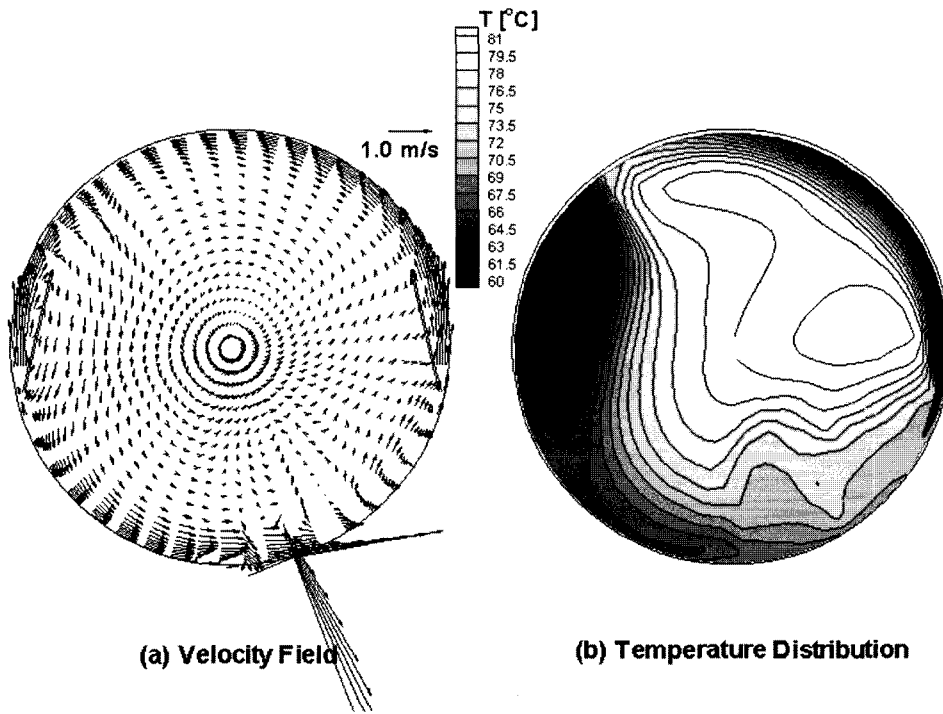


Fig. 7. Steady-State Simulation Results for the Wolsong 2/3/4 Moderator Using CFX-4; Cross-sectional View 1.418 Meters Away from One End Tubesheet

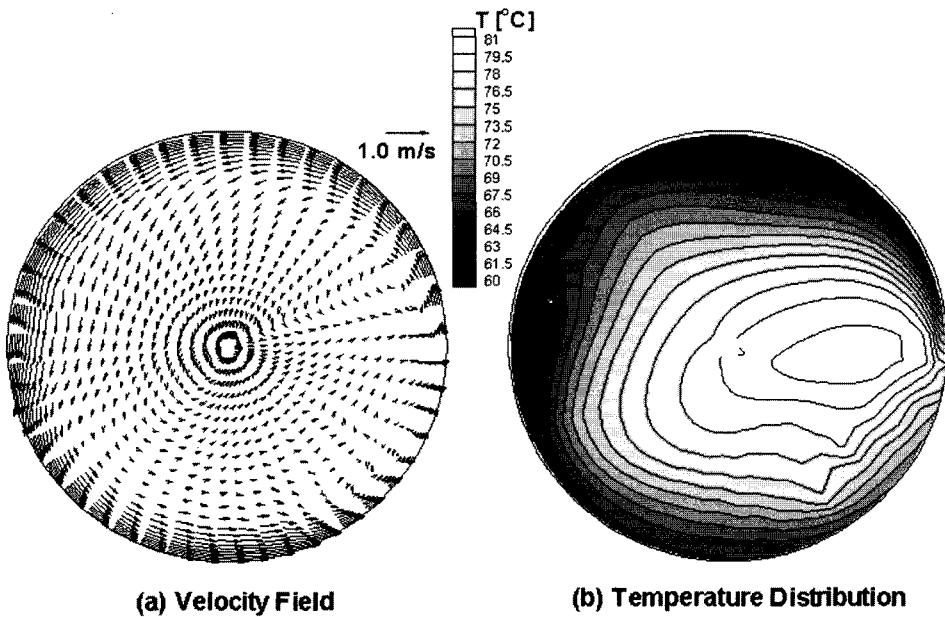


Fig. 8. Steady-State Simulation Results for the Wolsong 2/3/4 Moderator Using CFX-4; Cross-sectional View 3.0 Meters Away from One End Tubesheet

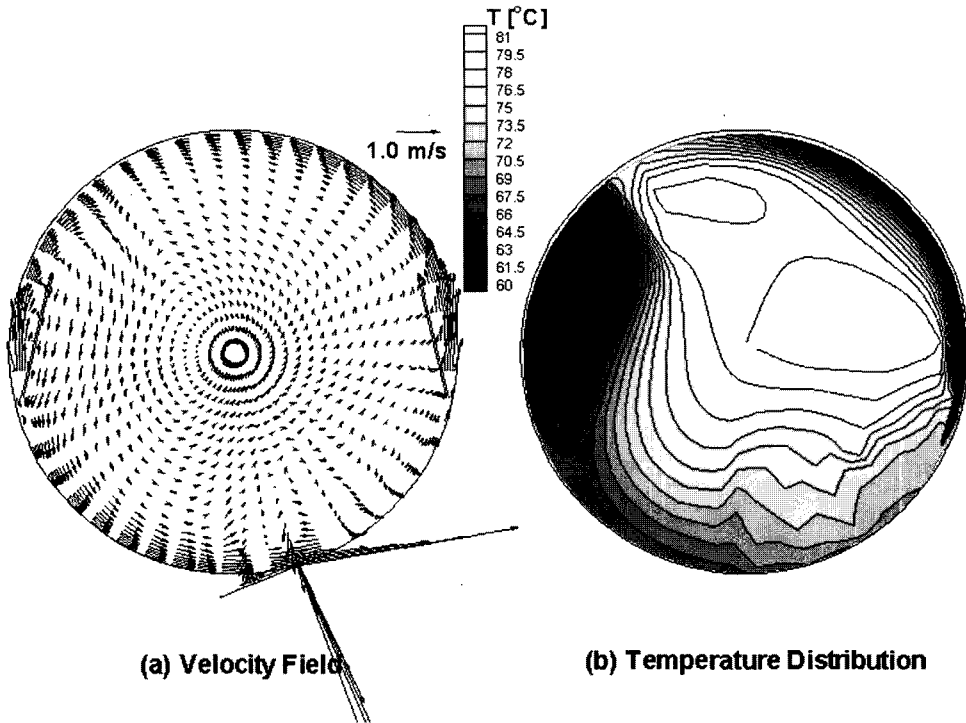


Fig. 9. Steady-State Simulation Results for the Wolsong 2/3/4 Moderator Using CFX-4; Cross-sectional View 4.582 Meters Away from One End Tubesheet

region, which is slightly tilted to one side from the vertical centerline.

Figure 8 shows the velocity vectors and temperature contours in the cross section of $z = 3.0$ m away from one end tubesheet. In this plane, neither the inlet nozzles nor the outlet port appears. In Fig. 8(a), the flow pattern of the reflector region is similar to Fig. 7(a), except that there is neither an inlet jet nor an exiting velocity vector. The jet reversal does not appear. In Fig. 8(b), the hottest spot is located at the upper center area of the core region, which tilts to one side from the vertical centerline.

Figure 9 represents the velocity field and temperature distribution in the x - y plane of $z = 4.582$ m away from one end tubesheet, where the two inlet nozzles and an outlet port appear. In Fig.

9(b), the hottest spot is located at the upper center area of the core region where the maximum temperature is 82.9°C .

Figure 10 shows the velocity vectors and temperature distribution in the y - z plane, which is 0.3 m away from the axis of the cylindrical calandria tank. From Fig. 10(a), it is shown that there is a relatively small fluid movement in the z -direction around the center region. Note that the vector length is clearly increased to present relatively smaller velocity vectors. Near the outlets at the bottom of the main-shell, the fluids move towards the closer outlet. In Figure 10(b), the isotherms at the lower part of the vessel indicate that the fluids in these areas are stratified. Note that the positions of the inlet nozzles are not symmetric across the central x - y plane ($z = 3.0$ m).

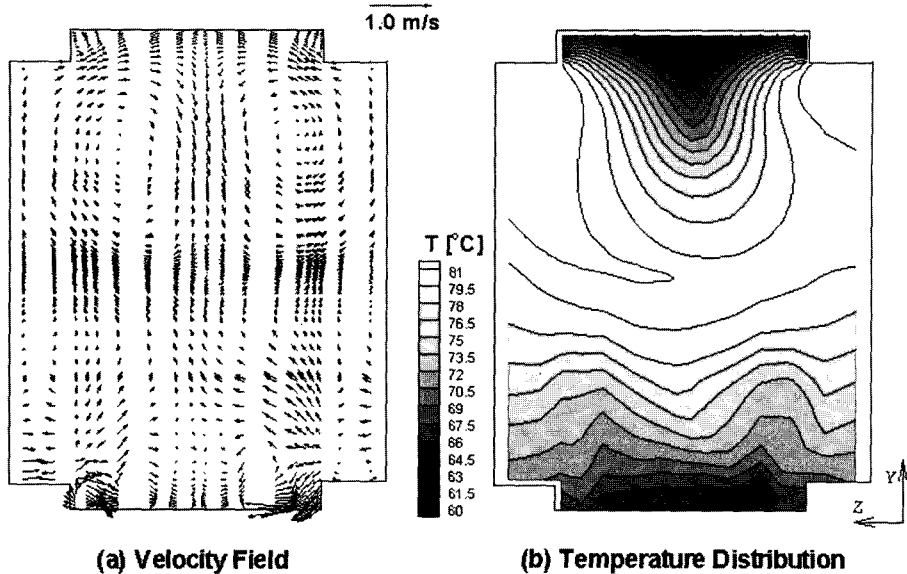


Fig. 10. Steady-State Simulation Results for the Wolsong 2/3/4 Moderator Using CFX-4; Side View for a Vertical Plane of $x = 0.3$ m

4. Conclusions

In this study, a CANDU moderator analysis model using CFX-4.4 is established and a simulation for predicting the local subcooling of the moderator in the vicinity of the calandria tubes in the CANDU6 reactor is performed. The temperature distributions and velocity fields of the simulation results are presented. The flow patterns of the constant- z slices containing the inlet nozzles and an outlet port (Fig. 7 & 9) are “mixed-type,” as observed in the 2-dimensional experimental investigations. With 103% full power for conservatism, the maximum temperature of the moderator is 82.9°C at the top of the core region. Considering the hydrostatic pressure change, the minimum subcooling is 24.8°C . With the initial condition obtained from this steady-state moderator analysis, transient analyses for some loss of coolant accidents with a coincident loss of emergency core cooling will be performed in a future study. Partial results of the transient analysis

for a selected LOCA can be found in C. Yoon et al. [9].

Even though the results of this analysis are reasonable, the analysis model has certain approximations that need to be examined further and possibly improved. Future studies would include the following.

- 1) In this study, the nozzles are simplified as a square block and inlet velocities are set uniform. A detailed nozzle modeling and sensitivity study of inlet velocity profiles on the simulation results is necessary and will be performed in future research.
- 2) A butterfly-shaped grid will be adopted in the next simulation model. Also, embedding the grid around inlet nozzles will be tried and tested, along with estimating the discretization error.
- 3) A 3-D hydraulic resistance correlation for the porous media approach will be developed using the experimental data for the flows across inclined tube banks in association with

the empirical correlation of cross flows.

- 4) The model has been validated against SPEL and STERN experimental data [10], which are basically 2-dimensional flow tests. A validation against 3-dimensional experimental data for CANDU moderator circulation should be performed as soon as this 3-dimensional experimental data is obtained.

Acknowledgment

This study has been carried out under the Nuclear Research and Development Program (Establishment of Safety Analysis System and Technology for CANDU Reactors) supported by the Korean Ministry of Science and Technology.

References

1. L.N. Carlucci and I. Cheung, "The Effects of Symmetric/Asymmetric Boundary Conditions on the Flow of an Internally Heated Fluid," *Numerical Methods for Partial Differential Equations*, 2, 47-61 (1986).
2. R.G. Huget, J.K. Szymanski, and W.I. Midvidy, "Status of Physical and Numerical Modelling of CANDU Moderator Circulation," *Proceedings of 10th Annual Conference of the Canadian Nuclear Society*, Ottawa (1989).
3. R.G. Huget, J.K. Szymanski, and W.I. Midvidy, "Experimental and Numerical Modelling of Combined Forced and Free Convection in a Complex Geometry with Internal Heat Generation," *Proceedings of 9th International Heat Transfer Conference*, Vol. 3, 327 (1990).
4. W.M. Collins, "PHOENICS2 Model Report for Wolsong 2/3/4 Moderator Circulation Analysis," Wolsong NPP 2/3/4, 86-03500-AR-053, Revision 0 (1995).
5. P. Seodijono, W.M. Collins, and T. De, "Moderator Analysis for In-Core and Out-of-Core Loss of Coolant Accident (LOCA)," Wolsong NPP 2/3/4, 86-03500-AR-052, Revision 0 (1995).
6. N.E. Todreas and M.S. Kazimi, *Nuclear System II: Elements of Thermal Hydraulic Design*, Chap. 5, Hemisphere Publishing Corporation (1990).
7. G.I. Hadaller, R.A. Fortman, J. Szymanski, W.I. Midvidy and D.J. Train, "Frictional Pressure Drop for Staggered and In Line Tube Bank with Large Pitch to Diameter Ratio," *Proceedings of 17th CNS Conference*, Fredericton, New Brunswick, Canada (1996).
8. K. Aydogdu, K.Y. Kim, and Y.I. Kim, "Radiation Heating Report," Wolsong NPP 2/3/4, 86-03320-AR-004, Revision 2 (1994).
9. Churl Yoon, Bo Wook Rhee, and Byung-Joo Min, "3-D CFD Analysis of the CANDU-6 Moderator Transient for the 35% RIH Break with Loss of ECC Injection," *The 10th International Topical Meeting on Nuclear Reactor Thermal Hydraulics (NURETH-10)*, Seoul, Korea, October (2003).
10. Churl Yoon, Bo Wook Rhee, and Byung-Joo Min, "Development and Validation of the 3-D CFD Model for CANDU-6 Moderator Temperature Predictions," Accepted for the publication in *Nuclear Technology*, vol. 148, no.3, 259-267 (2004).